C. R. Physique 20 (2019) 593–603

Contents lists available at ScienceDirect

Comptes Rendus Physique

www.sciencedirect.com

Evaluation of the effect of a phase-change material on the thermal response of a bizone building under the climatic conditions of Tunisia

Évaluation de l'effet d'un matériau à changement de phase sur la réponse thermique d'un bâtiment bi-zone dans les conditions climatiques de la Tunisie

Nour Ben Taher [b,*], Nour Lajimi [a], Noureddine Boukadida [b]

[a] *Laboratory of Metrology and Energy Systems, National School of Engineering of Monastir (ENIM), Tunisia*
[b] *High School of Sciences and Technology of Hammam Sousse (ESSTHS), Tunisia*

ARTICLE INFO

Article history:
Available online 10 April 2019

Keywords:
Building
Phase-change materials
Composite wall
Thermoelectricity

Mots-clés :
Bâtiment
Matériaux à changement de phase
Mur composite
Thermoélectricité

ABSTRACT

This paper extends the thermoelectric analogy method to study the thermal behavior of a concrete envelope of a dual-zone building containing microencapsulated phase-change material (PCM) and subjected to realistic climatic conditions based on weather data for a typical summer day in Tunisia. This work deals with a numerical study based on the nodal method to predict the effect of phase change on the thermal response as well as the energy flux reduction associated with the composite-envelope building.

RÉSUMÉ

Cet article traite la méthode de l'analogie thermoélectrique pour étudier le comportement thermique de l'enveloppe en béton d'un bâtiment à deux zones contenant un matériau à changement de phase (MCP) microencapsulé et soumis à des conditions climatiques réalistes basées sur des données météorologiques pour une journée d'été typique en Tunisie. Ce travail rapporte une étude numérique basée sur la méthode nodale pour prédire l'effet du changement de phase sur la réponse thermique ainsi que sur la réduction du flux d'énergie associée au bâtiment à enveloppe composite.

* Corresponding author.
E-mail addresses: noor.bentaher@yahoo.com (N. Ben Taher), nourlajimi@yahoo.fr (N. Lajimi), nournour.boukadida@gmail.com (N. Boukadida).

https://doi.org/10.1016/j.crhy.2019.01.004
1631-0705/

Nomenclature

c_p	specific heat capacity	J/(kg K)
$C_{i,j}$	conductive or convective coefficient between nodes i and j	W/K
E_r	energy flux reduction	%
f	decrement factor	
h	convective heat transfer coefficient	W/m^2 K
h_{sf}	latent heat of fusion	kJ/kg
k	thermal conductivity	W/(m K)
$K_{i,j}$	radiative coupling coefficient	W/K^4
$(mc)_i$	heat capacity	J/K
P	solar flux	W
q	heat flux density	W/m^2
t	time	h
T	real-time temperature	°C
T_{pc}	PCM phase change temperature	°C
ΔT_{pc}	PCM phase change temperature window	°C

Greek symbols

α	outer wall surface absorptivity	
ε	outer wall surface emissivity	
Φ_c	PCM volume fraction	
ϕ	time lag	h
ρ	density	kg/m^3

Subscripts

i	inner surface
i	number of the node
j	number of the node
o	outer surface
l	liquid phase
s	solid phase or shell

1. Introduction

The reduction of energy consumption in the building sector has become a top priority. The share of consumption of this sector is continuously increasing worldwide. In particular, climatic conditions generate a situation of discomfort, which requires the use of increasingly efficient air-conditioning systems. Special attention should be drawn to improve the thermal quality of the building envelope with real consideration of the climate specificity.

To assure comfort conditions, many solutions can be presented, such as insulation of walls and roofs [1], using light colors on the external surfaces [2], and the use of energy storage devices in the building structure.

Cabeza et al. have experimentally evaluated the energy savings that can be achieved through thermal insulation in a continental Mediterranean climate [3]. Their results showed that good insulation is crucial for reducing energy consumption during both summer and winter periods. Di Perna et al. concluded that the use of high thermal inertia walls in buildings generally contributes to reducing energy requirements for both heating and cooling [4].

In recent decades, attention has been drawn to the use of phase-change materials (PCMs) in the building. They are considered a good way to increase the thermal inertia of envelopes. Several experimental studies have been conducted to demonstrate the benefits of using PCMs. Cabeza et al. developed and tested improved concrete containing microencapsulated PCMs. Their experiments were performed to compare the behavior of new composite materials with conventional concrete [5]. The results of the experimental measurements showed that the new innovative concrete improved thermal inertia and decreased the inner temperatures of the walls. In a similar approach, Castell et al. [6] evaluated the behavior of macro-encapsulated PCMs in brick construction for passive summer cooling. The experiments were conducted under real-world weather conditions and the results demonstrated using PCMs reduces indoor temperature fluctuations and energy consumption.

Kissock and Limas simulated time-dependent one-dimensional heat transfer in a 30.4-cm-thick south-facing multilayered wall in Dayton, Ohio [7], consisting of an insulating layer sandwiched between two concrete layers imbibed with a paraffin PCM rate of 10%. The effective specific heat of the wall was determined by a weighted average of the specific heat of the concrete and that of PCMs, which depends on temperature. The authors focused on the phase change peak of the PCM specific heat curve at the set indoor temperature. They found that the maximum and annual cooling loads were reduced by 19% and 13%, respectively, and the maximum and annual heating loads were reduced by only 11% and 1%, respectively.

Zwanzig et al. simulated a monozone building in Minneapolis, MN, Louisville, KY, and Miami, Florida, consisting of 15.3-cm-thick walls and of a 12.4-cm-thick roof of conventional multilayer construction [8]. The roof and the vertical walls contained a 1.3-cm-thick layer of gypsum wallboard impregnated with a 25% paraffin PCM, whose phase-change temperature is between 25 and 27.5 °C. The authors showed that adding PCMs to the walls and roof reduces the building heat load during the cooling season (summer) more than during the heating season (winter).

Alexander M. Thiele et al. simulated the time-dependent three-dimensional heat transfer in a vertical composite wall [9] consisting of monodisperse or polydisperse microcapsules of PCM randomly distributed in a continuous matrix of concrete [10,11]. They showed that the temporal evolution of temperature and the heat flux predicted within a homogeneous material with appropriate effective thermal properties agreed very well with that within a heterogeneous material with discrete core, shell, and matrix materials.

Research works in the building physics in Tunisia are scarce despite the increase in energy consumption. The building sector (covering the residential and tertiary buildings) is currently the third final energy consumption (of which the part of cooling and heating is very large) and it will occupy the first position in a few years according to the National Agency for Energy Management (ANME Tunisia).

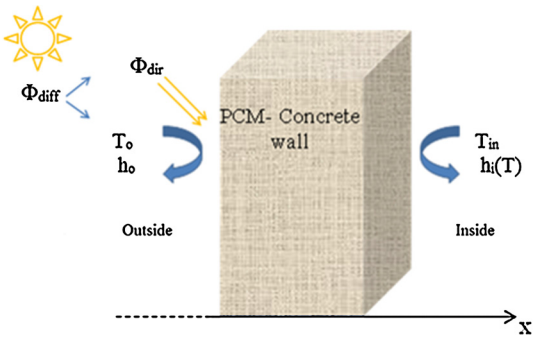

Fig. 1. Schematic of a microencapsulated PCM/concrete wall subjected to an outdoor air temperature $T_o(t)$ and a solar flux at the outside surface ($x = 0$ m).

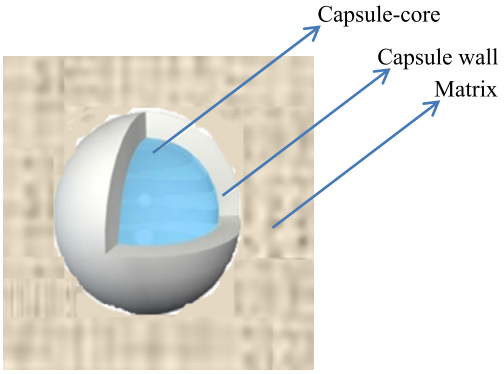

Fig. 2. Schematic of a microcapsule PCM integrated in a concrete matrix (adapted from [21]).

In recent constructions in Tunisia, there is no special attention paid to improving the thermal quality of the building envelope, but some studies were concerned with the effect of thermal insulation on energy savings.

Daouas [12] estimated the yearly cooling and heating transmission loads for two types of insulation materials and determined the optimum insulation thickness, the resulting energy savings, and payback period. In [13], a multi-alveolar structure is integrated in the common wall of a bi-zone building. The authors showed that this structure is equivalent to a polystyrene layer and it allowed one to reduce the heat power required in winter.

Based on the literature, the integration of microencapsulated PCMs into building materials has been studied in several works but, under the climatic conditions of Tunisia, this technique is scarce. In our work, we have studied numerically the microencapsulation of PCM and we have chosen a PCM whose melting temperature is close to the summer temperature comfort (this temperature is fixed at 26 °C), which is integrated in a concrete layer (a material that is little used in the construction of Tunisian buildings).

We simulate in the present paper the one-dimensional heat transfer through a concrete wall containing microencapsulated PCMs under climatic conditions in the region of Sousse, Tunisia. We study the effect of adding microencapsulated phase-change materials and of the volume fraction of this material (PCM) on the thermal response of a dual-zone building wall.

2. Theoretical modeling

2.1. Position of the problem

In this work, we are interested in evaluating the thermal response of a microencapsulated PCM/concrete composite wall of a dual-zone building. This novel procedure accurately accounts for the effects of phase change on the thermal load through building envelopes containing PCM that are subjected to realistic outdoor air temperatures and solar flux measured by the meteorological station of Sousse, Tunisia (Fig. 1). The three materials correspond to a commercially available paraffin RT25 [14], high-density polyethylene (HDPE) [15], and concrete [16], respectively (Fig. 2).

The microcapsules of PCM are randomly distributed in a continuous matrix of concrete, and the density, the thermal conductivity, the specific heat of PCM, polymer shell, and matrix are given in Table 1 [14–16].

2.2. Formulation of the problem

In this work we have assumed the following assumptions:

Table 1
Thermophysical properties of PCMs, high-density polyethylene (HDPE), and concrete.

Material	Thermophysical properties		
	ρ (kg/m^3)	c_p (J/kg K)	K (W/m K)
PCM (paraffin RT27)	767	2100	0.185
HDPE	930	2250	0.49
Concrete	2300	880	1.4

- the heat transfer is unidirectional;
- the air is considered as a perfect transparent gas;
- the thermophysical properties of each material are constant.

The heat transfer by conduction through a wall, in the case without a heat source, is described by:

$$\rho c_p \frac{\mathrm{d}T}{\mathrm{d}t} = k \frac{\mathrm{d}^2 T}{\mathrm{d}x^2} \tag{1}$$

where ρ, c_p, and k are the density, the thermal conductivity, and the specific heat capacity of the material, respectively.

Modified PCM/concrete materials can be considered as two-phase materials consisting of reference concrete and PCM particles. In this case, the thermal conductivity of the composite material can be predicted from homogenization schemes as a function of the thermal conductivities of the two phases (concrete and PCM) and of their volume fractions.

The expression of the effective thermal conductivity of the composite wall was accurately predicted by Felske's model [9,17]:

$$k_{\mathrm{eff}} = \frac{2k_{\mathrm{m}}(1-\phi_{\mathrm{c}}-\phi_{\mathrm{s}})(3+2\frac{\phi_{\mathrm{s}}}{\phi_{\mathrm{c}}}+\frac{\phi_{\mathrm{s}}k_{\mathrm{c}}}{\phi_{\mathrm{c}}k_{\mathrm{s}}})+(1+2\phi_{\mathrm{c}}+2\phi_{\mathrm{s}})[(3+\frac{\phi_{\mathrm{s}}}{\phi_{\mathrm{c}}})k_{\mathrm{c}}+2\frac{\phi_{\mathrm{s}}k_{\mathrm{s}}}{\phi_{\mathrm{c}}}]}{(2+\phi_{\mathrm{s}}+\phi_{\mathrm{c}})(3+2\frac{\phi_{\mathrm{s}}}{\phi_{\mathrm{c}}}+\frac{\phi_{\mathrm{s}}k_{\mathrm{c}}}{\phi_{\mathrm{c}}k_{\mathrm{s}}})+(1-\phi_{\mathrm{c}}-\phi_{\mathrm{s}})[(3+\frac{\phi_{\mathrm{s}}}{\phi_{\mathrm{c}}})\frac{k_{\mathrm{c}}}{k_{\mathrm{m}}}+2\frac{\phi_{\mathrm{s}}k_{\mathrm{s}}}{\phi_{\mathrm{c}}k_{\mathrm{m}}}]} \tag{2}$$

k_{c}, k_{s}, and k_{m} are the thermal conductivities of the core (PCM), the shell (HDPE), and the matrix (concrete), respectively, ϕ_{c} and ϕ_{s} are the core and shell volume fractions.

The effective volumetric heat capacity is given by [9],

$$(\rho c_p)_{\mathrm{eff}}(T) = \phi_{\mathrm{c}}(\rho c_p)_{\mathrm{c}}(T) + \phi_{\mathrm{s}}(\rho c_p)_{\mathrm{s}} + (1-\phi_{\mathrm{c}}-\phi_{\mathrm{s}})(\rho c_p)_{\mathrm{m}} \tag{3}$$

It depends on the temperature [9], as it is written below:

$$\begin{cases} (\rho c_p)_{\mathrm{eff,s}} & \text{for } T < T_{\mathrm{pc}} - \Delta T_{\mathrm{pc}}/2 \\ (\rho c_p)_{\mathrm{eff}}(T) = (\rho c_p)_{\mathrm{eff,s}} + \phi_{\mathrm{c}} \frac{\rho_{\mathrm{c,s}} h_{\mathrm{sf}}}{\Delta T_{\mathrm{pc}}} & \text{for } T_{\mathrm{pc}} - \Delta T_{\mathrm{pc}}/2 \le T \le T_{\mathrm{pc}} + \Delta T_{\mathrm{pc}}/2 \\ (\rho c_p)_{\mathrm{eff,l}} & \text{for } T > T_{\mathrm{pc}} + \Delta T_{\mathrm{pc}}/2 \end{cases} \tag{4}$$

where T_{pc}, ΔT_{pc}, and h_{sf} are the phase-change temperature (25.85 °C), the phase-change temperature window (ΔT_{pc} denotes the interval $(T_{\mathrm{l}} - T_{\mathrm{s}})$, which is equal to 3 °C) and the latent heat of fusion (which is taken to be equal to 232 kJ/kg), respectively.

2.3. Discretization of the model and solving method

We used the nodal method as a numerical method that is frequently used to study the building's thermal behavior; it integrates the concept of the fictitious node and does not require a refined mesh, especially in thermal buildings. It consists in splitting the system into multiple elements; each element is represented by a node that is affected by temperature and the thermo-physical properties of the element. This model is divided into 81 nodes. For more details, the reader can refer to [18]. To solve this problem, the thermoelectricity analogy method is used [13] and is described in Fig. 3.

The mathematical model based on the balance equation is written as:

$$(mc)_i \frac{\mathrm{d}T_i}{\mathrm{d}t} = \sum_{j=1,n} C_{i,j}(T_j - T_i) + \sum_{j=1,n} K_{i,j}\left(T_j^4 - T_i^4\right) + P_i(t) \tag{5}$$

where $(mc)_i$, T_i and $C_{i,j}$, $P_i(t)$ are the specific heat capacity, the real-time temperature, the conductive or convective coefficient between nodes i and j, the Solar flux absorbed at time t by node i, respectively. $K_{i,j}$ is the radiative coupling coefficient between i and j.

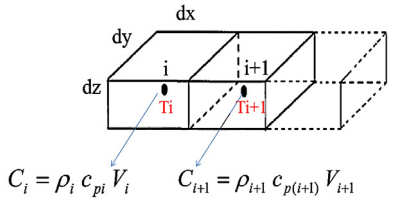

(a)

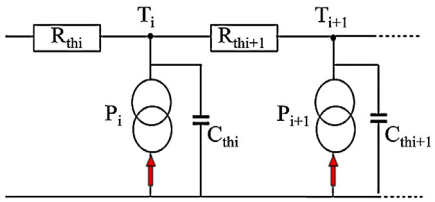

(b)

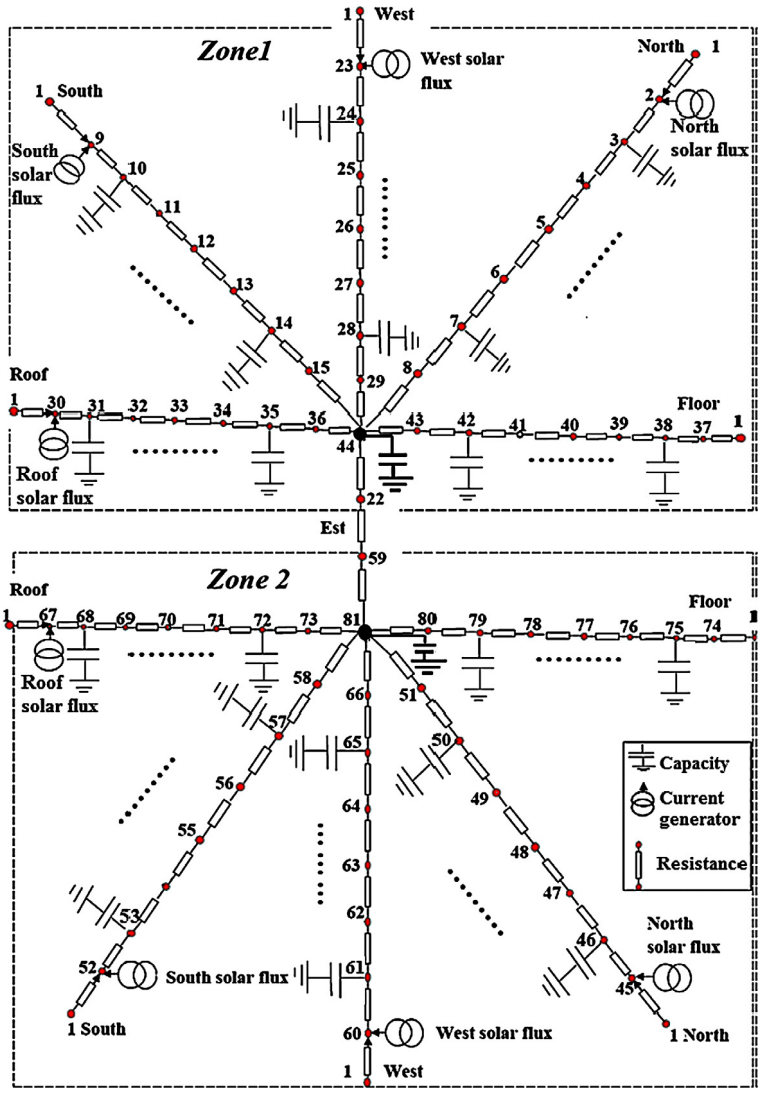

(c)

Fig. 3. (a) Nodal decomposition of the system; (b) conductance network creation; (c) thermoelectricity analogy model used for the bizone building.

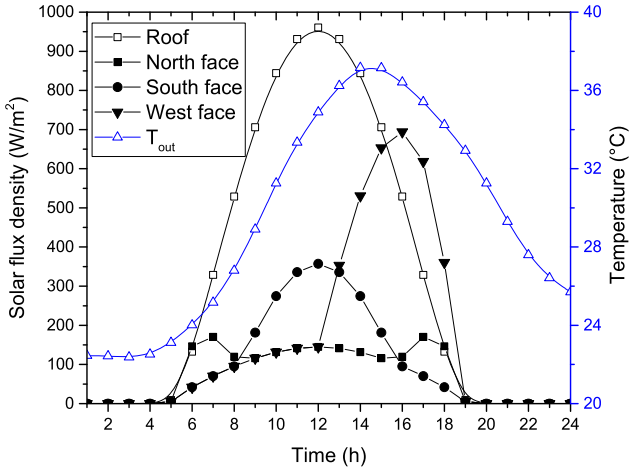

Fig. 4. Outdoor air temperature and solar radiation heat flux density incident upon north-, south-, west-facing vertical walls and roof in July in Sousse.

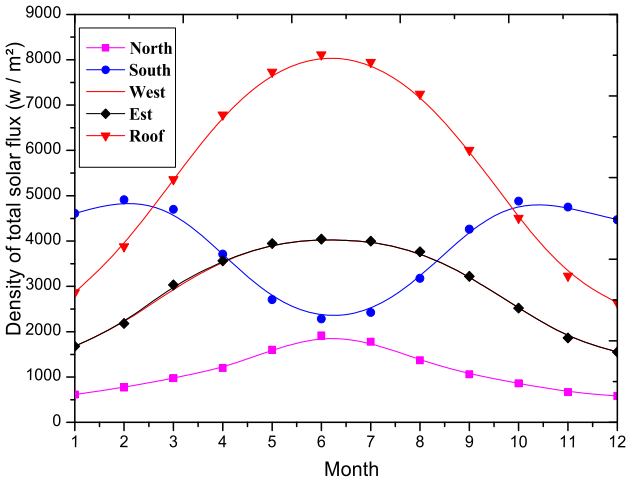

Fig. 5. Annual evolution of the total solar flux density received by different faces.

2.4. Boundary and initial conditions

The outside meteorological air temperature values are provided by the local weather station of Sousse, Tunisia. The direct and the diffuse solar density fluxes are calculated hourly, on the 15th day, which is considered as a typical day of the month.

For each orientation of the wall, Fig. 4 represents the time-dependent outdoor air temperature and the incident solar flux density on the outer face on a summer day. Fig. 5 plots the annual evolution of the total solar flux density for the roof and each orientation in Sousse (Tunisia).

Whatever the orientation, the average coefficients of emission and absorption of the outer and inner surfaces of each wall are set at $\overline{\varepsilon} = 0.9$ and $\overline{\alpha} = 0.8$, respectively.

The heat transfer coefficient at the outer and inner surfaces of the vertical walls are $h_o = 11$ W/(m^2 K) and $h_i(T)$, respectively.

Fig. 4 shows that the faces that receive the highest amounts of solar radiation are the west-facing wall (with a maximum of 694 W/m^2, Fig. 4c) and the roof (a maximum of 960 W/m^2, Fig. 4d).

Fig. 5 plots the annual total solar flux density received by the different faces and shows that, throughout the year, the roof receives a very large amount of solar flux that can reach 8000 W/m^2.

From these results obtained by our simulation, we attach a great importance to studying the thermal behavior of the roof and of the west-facing wall by adding microencapsulated PCMs.

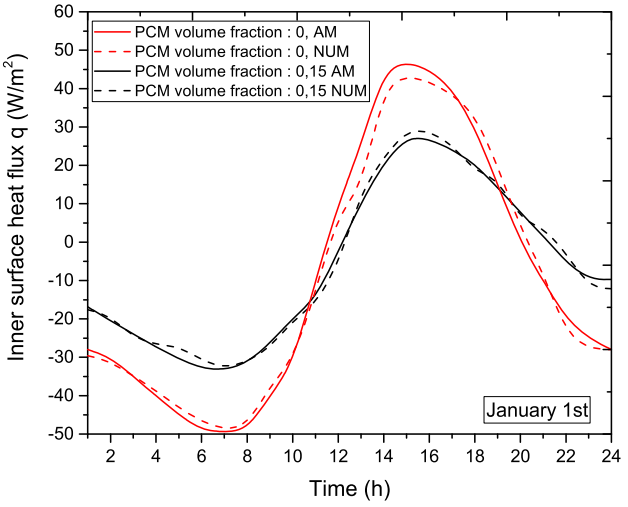

Fig. 6. Comparison between inner heat flux densities as a function of the PCM volume fraction resulting from the FORTRAN simulation based on the thermoelectricity analogy method and the modified admittance method [19] for a wall subjected to a realistic air temperature representative of 1 January in California.

3. Validation

The accuracy of our model is assessed by comparing the evolution of the inner surface heat flux density ($q(t)$) as a function of time for a single wall containing PCMs resulting from our FORTRAN simulation based on the thermoelectricity analogy method with that obtained with the modified admittance method proposed by Alexander M. Thiele et al. [19]. The single composite wall is subjected to a realistic air temperature representative of 1 January in a Californian climate. The studied wall is a single layer concrete slab of thickness 10 cm and subjected to convection to indoor air at a constant temperature $T_{\text{in}} = 20\,^{\circ}\text{C}$ with a heat transfer coefficient $h_{\text{i}} = 7.7$ W/(m^2 K) at the inner wall surface and to an outdoor air temperature with a heat transfer coefficient $h_{\text{o}} = 25$ W/(m^2 K) at the outer wall surface [19]. The wall was also subjected to a solar radiation flux at the outer wall surface, which was calculated by our simulation for a latitude in California (36.46 N) and for 1 January.

The phase change temperature window (ΔT_{pc}) and the PCMs' latent heat of fusion (h_{sf}) were taken as 8 °C and 180 kJ/kg, respectively, characteristic of PureTemp 20 [20]. The total hemispherical solar absorptivity of the outer wall surface was taken as 0.26, corresponding to that of white paint. We considered the same assumptions (1), (2), and (3) in [19].

Fig. 6 plots the inner wall surface heat flux $q(t)$ as a function of time predicted numerically for a concrete wall containing 0, 15, and 30 vol.% of microencapsulated PCMs on 1 January. The curves corresponding to the work of A.M. Thiele et al. based on the modified admittance method (noted AM) and on ours (NUM) are appreciably close.

4. Results and discussion

In this section, we will compare the thermal response of the roof with that of the west-facing wall.

As a first result, for 1 January, Figs. 7a and b illustrate the inner wall surface temperature as a function of time for a concrete wall containing microencapsulated PCMs with a volume fraction ϕ_{c} ranging from 0 to 30% and subjected to a realistic outdoor air temperature.

Whatever the face (roof or west face), it is shown that the thermal oscillation amplitude decreases with increasing the PCM volume fraction ϕ_{c}. For the roof (Fig. 7a), the inner surface temperature stabilizes for $\phi_{\text{c}} = 0.2$, and for $\phi_{\text{c}} = 0.3$ it takes values between 29.5 °C and 30.4 ° C. For the west face (Fig. 7b), the inner surface temperature becomes slightly fluctuating for $\phi_{\text{c}} = 0.3$ (between 29.2 °C and 32.4 °C), but it is more fluctuating than the one corresponding to the roof.

Figs. 8a and b plot the inner wall surface heat flux $q(t)$ as a function of time for a concrete wall containing microencapsulated PCMs with a volume fraction ϕ_{c} ranging from 0 to 30%. For both walls (roof and west face), adding microencapsulated PCMs decreases the amplitude of oscillation of the inner wall heat flux $q(t)$. We note that, for the roof (Fig. 8a), an increase of ϕ_{c} up to 0.3 causes a decrease in the amplitude of the oscillation of the inner surface heat flux from 44,8 W/m^2 to 30.58 W/m^2. For the west face (Fig. 8b), the same variation in ϕ_{c} results in a reduction from 422 W/m^2 to 293 W/m^2.

Fig. 9 plots the decrement factor as a function of the microencapsulated PCM volume fraction with a volume fraction ϕ_{c} ranging from 0 to 30%. This factor corresponds to the reduction in cyclical temperature on the inner surface compared to the outer surface. Many studies defined this factor as the ratio of the amplitudes of oscillation in temperature at the inner and outer surfaces of the wall, expressed as [19] $f = \frac{T_{L,\max} - T_{L,\min}}{T_{\text{o},\max} - T_{\text{o},\min}}$ where $T_{L,\max}$ and $T_{\text{o},\max}$ are the maximums of the inner

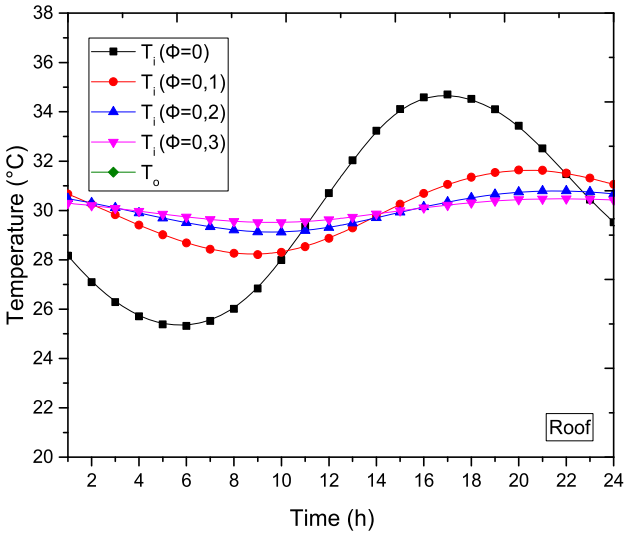

(a)

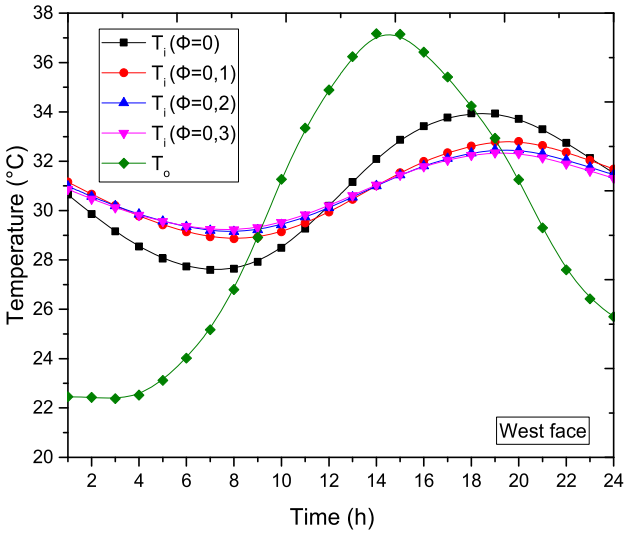

(b)

Fig. 7. Inner surface temperature for a roof and a west-facing wall in July in Sousse.

and outer surfaces of the wall, respectively, and $T_{L,\min}$ and $T_{o,\min}$ are the minimums of the inner and outer surfaces of the wall, respectively.

One can see that the decrement factor (f) decreases with ϕ_c. Adding PCMs has the most pronounced effect when this material is incorporated into the roof. In this case, f drops from 33.47% to 9.83%, while that corresponding to the west-facing wall decreases from 14% to 1%.

Several studies defined the time lag (ϕ), which corresponds to the time delay due to the thermal mass, as the difference between the time (in hours) when the inner and outer wall surface temperatures reach their respective maxima [19].

Fig. 10 plots the time lag (ϕ) and shows that this parameter increases with ϕ_c. Adding microencapsulated PCMs has an important effect on the predicted time lag in the case of the microencapsulated PCM/concrete roof where it increases from 2 to 7 h compared with that corresponding to the microencapsulated PCM/concrete west-facing wall, which increases from 2 to 5 h.

Fig. 11 plots the evolution with ϕ_c of the energy flux reduction (E_r), which is defined by

$$E_r = \frac{Q_{L,m} - Q_L}{Q_{L,m}}$$

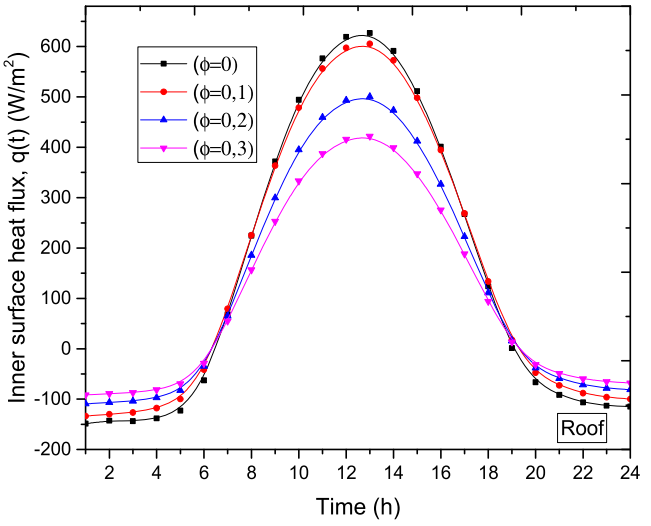

(a)

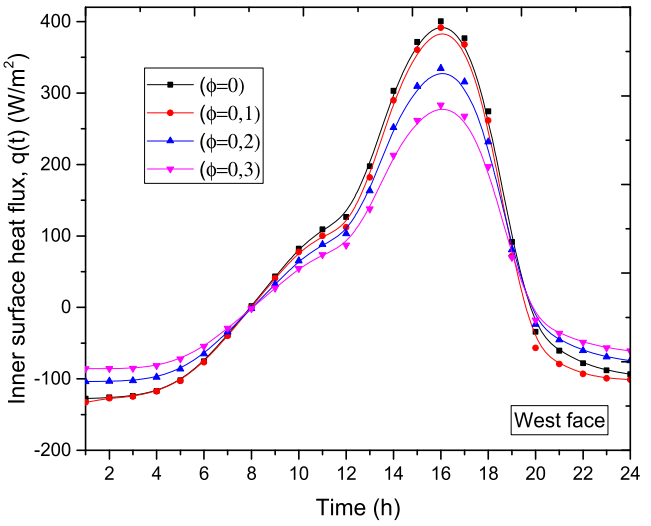

(b)

Fig. 8. Inner surface density heat flux $q(t)$ as a function of time for a simple layer containing up to 30% of PCM.

where $Q_{L,m}$ and (Q_L) are the daily energy flux densities (in $\mathrm{J\,m^{-2}}$) through the wall without $(Q_{L,m})$ and with (Q_L) microencapsulated PCMs. They are expressed as:

$$Q_{L,m} = \int_0^{24\mathrm{h}} \left|q_{L,m}(t)\right| \mathrm{d}t \quad \text{and} \quad Q_L = \int_0^{24\mathrm{h}} \left|q_L(t)\right| \mathrm{d}t$$

where $q_{L,m}(t)$ and $q_L(t)$ are the conductive heat flux densities at the inner wall surface without and with microencapsulated PCMs, respectively.

The absolute values of the heat fluxes density $q_{L,m}(t)$ and $q_L(t)$ were considered to account for the fact that there is an energy cost associated with maintaining the indoor temperature at a setpoint temperature regardless of the direction of the heat flux across the wall.

Fig. 11 shows that E_r increases linearly with increasing ϕ_c due to the associated increase in thermal resistance and sensible heat storage of the wall, but we note that adding microencapsulated PCMs has a slightly larger impact on E_r, which increases from 0 to 32.2% when the PCM is integrated in the roof, while it reaches 28.7% in the case of the west-facing composite wall.

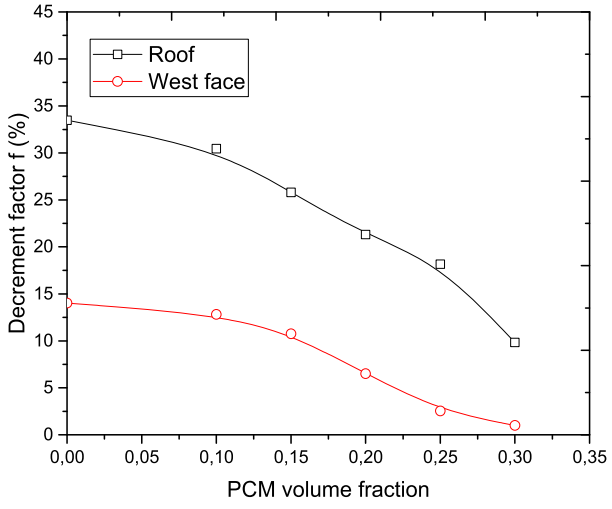

Fig. 9. Decrement factor (f) as function of PCM volume fraction for a composite layer.

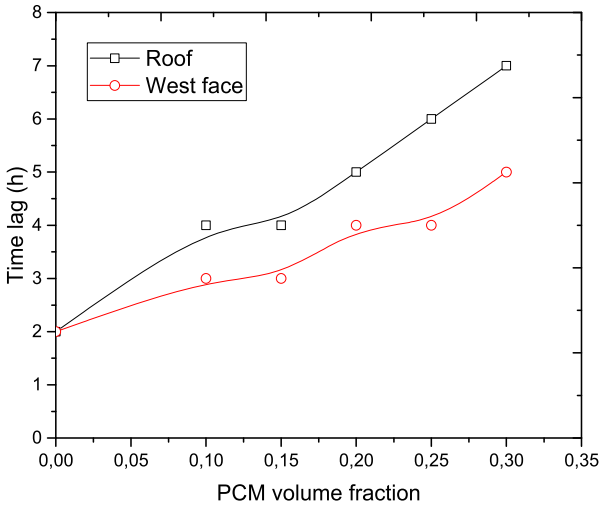

Fig. 10. Time lag ϕ as a function of the PCM volume fraction for a composite wall subjected to a realistic sol–air temperature representative of 15 July in Sousse (Tunisia).

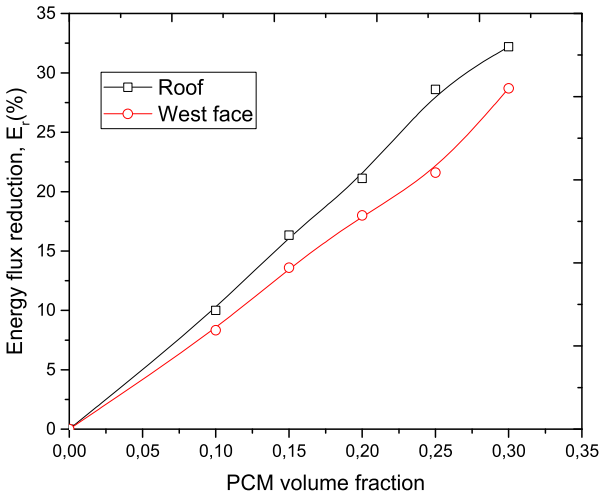

Fig. 11. Energy flux reduction E_r as a function of the PCM volume fraction for a composite wall subjected to a realistic sol–air temperature representative of 15 July in Sousse (Tunisia).

5. Conclusion

This study extended the thermoelectricity analogy method to account for the effects of phase change on the thermal load passing through single building envelopes subjected to realistic weather conditions in Sousse (Tunisia). We performed a comparative study between the effect of adding PCMs in the roof and in the west-facing wall. The proposed method predicted the inner surface temperature, the inner surface heat flux, the decrement factor and time lag, and also the energy flux reduction (E_r) associated with adding PCMs to building. This study concluded that adding microencapsulated PCMs to concrete walls and increasing the PCM volume fraction substantially reduced and delayed the thermal load of the building.

The simplicity of the used model based on the thermoelectricity method and validated with an analytical method facilitated the prediction and the evaluation of the energy benefits of PCM/concrete composite walls, and the results led us to take an interest in future studies to evaluate energy consumption and to examine the cost-saving potential of incorporating PCM into the building roof.

An experimental investigation of a PCM/concrete composite wall under the Tunisian climate will be our future trend in order to validate our numerical findings.

References

[1] G. Barrios, G. Huelsz, J. Rojas, Thermal performance of envelope wall/roofs of intermittent air-conditioned rooms, Appl. Therm. Eng. 40 (2012) 1–7.
[2] A.D. Granja, L.C. Labakiny, Influence of external surface color on the periodic heat flow through a flat solid roof with variable thermal resistance, Int. J. Energy Res. 27 (2003) 771–779.
[3] L.F. Cabeza, A. Castell, M. Medrano, I. Martorell, G. Pérez, I. Fernández, Experimental study on the performance of insulation materials in Mediterranean construction, Energy Build. 42 (5) (May 2010) 630–636.
[4] C. Di Perna, F. Stazi, A. Ursini Casalena, M. D'Orazio, Influence of the internal inertia of the building envelope on summertime comfort in buildings with high internal heat loads, Energy Build. 43 (1) (2011) 200–206.
[5] L.F. Cabeza, C. Castellón, M. Nogués, M. Medrano, R. Leppers, O. Zubillaga, Use of microencapsulated PCM in concrete walls for energy savings, Energy Build. 39 (2) (February 2007) 113–119.
[6] A. Castell, I. Martorell, M. Medrano, G. Pérez, L.F. Cabeza, Experimental study of using PCM in brick constructive solutions for passive cooling, Energy Build. 42 (4) (April 2010) 534–540.
[7] K. Kissock, S. Limas, Diurnal load reduction through phase-change building components, ASHRAE Trans. (2006) 509–517.
[8] S.D. Zwanzig, Y. Lian, E.G. Brehob, Numerical simulation of phase-change material composite wallboard in a multi-layered building envelope, Energy Convers. Manag. 69 (2013) 27–40.
[9] A.M. Thiele, A. Jamet, G. Sant, L. Pilon, Annual energy analysis of concrete containing phase-change materials for building envelope, Energy Convers. Manag. 103 (2015) 374–386.
[10] A.M. Thiele, G. Sant, L. Pilon, Diurnal thermal analysis of microencapsulated PCM/concrete walls, Energy Convers. Manag. 93 (2015) 215–227.
[11] A.M. Thiele, A. Kumar, G. Sant, L. Pilon, Effective thermal conductivity of three component composites containing spherical capsules, Int. J. Heat Mass Transf. 73 (2014) 177–185.
[12] N. Daouas, Impact of external longwave radiation on optimum insulation thickness in Tunisian building roofs based on a dynamic analytical model, Appl. Energy 177 (2016) 136–148.
[13] N. Lajimi, N. Boukadida, Numerical study of the thermal behavior of bi-zone buildings, C. R. Physique 16 (8) (2015) 708–720.
[14] P.H. Biwole, P. Eclache, F. Kuznik, Phase-change materials to improve solar panel's performance, Energy Build. 62 (2013) 59–67.
[15] Typical Engineering Properties of High Density Polyethylene, Technical Report, INEOS Olefins & Polymers, League City, TX, USA, 2009.
[16] F.P. Incropera, A.S. Lavine, D.P. DeWitt, Fundamentals of Heat and Mass Transfer, John Wiley & Sons, New York, 2011.
[17] J.D. Felske, Effective thermal conductivity of composite spheres in a continuous medium with contact resistance, Int. J. Heat Mass Transf. 47 (2004) 3459–3461.
[18] H. Boyer, J.-P. Chabriat, C. Tourr, J. Brau, Thermal building simulation and computer generation of nodal models, Build. Environ. 31 (3) (1996) 207–214.
[19] A.M. Thiele, R.S. Ligett, G. Sant, L. Pilon, Simple thermal evaluation of building envelopes containing phase-change materials using a modified admittance method, Energy Build. 145 (2017) 238–250.
[20] T. Khadiran, M.Z. Hussein, Z. Zainal, R. Rusli, Encapsulation techniques for organic phase change materials as thermal energy storage medium: a review, Sol. Energy Mater. Sol. Cells 143 (2015) 78–98.
[21] PureTemp 20 Technical Information, Technical Report, Entropy Solutions Inc., Minneapolis, MN, USA, 2011.